Improved Tissue Phantoms for Experimental Validation of Microwave Breast Cancer Detection

Emily Porter, Jules Fakhoury, Razvan Oprisor, Mark Coates and Milica Popović

Department of Electrical and Computer Engineering, McGill University
3480 University Street, Montreal, QC, Canada
{emily.porter, jules.fakhoury, razvan.oprisor}@mail.mcgill.ca
{mark.coates, milica.popovich}@mcgill.ca

***Abstract*— This paper presents a methodology for constructing realistic breast phantoms for use in microwave detection of breast cancer. Phantoms for fat, skin, gland and tumour are made from a combination of everyday chemicals. The dielectric permittivity and conductivity of the phantoms are measured at microwave frequencies. Finally, we describe a procedure to combine the four phantom tissue types into a single breast phantom that is sufficiently realistic, both in terms of dielectric properties and physiological structure, to be used in experiments designed to assess the performance of microwave breast cancer detection techniques.**

***Index Terms*— Breast cancer detection, microwave imaging, tissue phantoms.**

I. Introduction

Microwave imaging of the breast, intensely researched in the past decade, assumes a difference in the dielectric properties between healthy breast tissue and tumour tissue at microwave frequencies [1]. Realistic breast models, also called phantoms, which mimic the dielectric properties of actual human breasts, are needed in order to test and further develop microwave imaging technologies.

Recently, two studies have been conducted which characterized the microwave dielectric properties of healthy and malignant breast tissue [2], [3]. These provided the most comprehensive set of measurements of the permittivity and conductivity of different breast tissues available to date and, therefore, make a good starting point for construction of tissue phantoms. In [4], an oil-in-gelatin mixture is used as a phantom material and it is shown that with varying concentrations, materials with a large range of dielectric properties can be obtained.

In this paper, we present a method for constructing breast phantoms with dielectric properties that mimic those of actual breast tissue. For the phantoms to be as realistic as possible, four different tissue-mimicking models are made: fat, skin, glands and tumour. Here, we build on the procedure suggested for preparing tissue-mimicking materials in [4] by identifying the specific concentrations of chemicals that lead to phantoms with dielectric properties that closely fit those of each of the four tissue types. Multiple phantoms are made using these sets of chemical concentrations and the permittivity and conductivity of each is measured from 200 MHz to 6 GHz. Finally, we propose techniques that allow us to incorporate the four phantom types into one stable, hemispherical breast model. The resulting breast phantom consists of a 2-mm layer of skin enclosing a mixture of adipose tissue, various sized glands, as well as (possibly) one or more tumours of different sizes.

II. Methodology

The construction of the breast phantoms involved three main steps: construction of the individual tissue phantoms from the chemical mixtures, measurements of their respective dielectric properties, and, finally, merging of the four different tissue types into a single complete breast model.

A. Step 1: Mixture of Tissue Phantoms

The first step in the construction process is to make four phantom types (fat, skin, gland and tumour) that have electrical properties in the microwave range similar to those of human breast tissue. In addition, the choice of materials was driven by a few other advantageous factors: the materials should be low in cost, easy to obtain (off-the-shelf) and stable over long periods of storage time. The phantoms are made from a mixture of gelatin and oil (50% safflower oil and 50% kerosene) [4]. The complete list of ingredients and the amounts or concentrations used for each hemispherical (radius = 6.5 cm) phantom type are given in Table I.

TABLE I
List of ingredients and the amount used for each tissue phantom

	Amount Used			
	Fat	Gland	Skin	Tumour
p-toluic acid (g)	0. 133	0.253	0.294	0.346
n-propanol (mL)	6.96	12.71	28.69	17.00
deionized water (mL)	132.7	241.9	279.5	328.0
200 Bloom gelatin (g)	24.32	43.27	50.02	58.67
Formaldehyde (37% by weight) (g)	1.53	2.74	3.33	3.72
oil (mL)	265.6	141.5	98.6	38.4
Ultra Ivory detergent (mL)	12.00	6.79	5.86	2.00

The chemicals are mixed using the same technique as has been suggested in [4]. Once the chemicals are mixed, it can take 1-2 days for the phantoms to solidify. After this time, they can be removed from the container they were allowed to set in (in the case of our work, a breast-shaped bowl) and will keep their shape. However, to ensure maximum shelf-life, the phantoms should be protected from moisture loss by thin plastic wraps or by placing them in air-tight containers. If they are not properly stored, the phantoms can become dehydrated, with significant change of dielectric properties.

B. Step 2: Measurement of Phantom's Dielectric Properties

Once the phantoms were allowed to solidify, the dielectric properties were tested. The measurements for the conductivity and relative permittivity for each phantom type were made at room temperature using an HP 85070B dielectric probe attached to a vector network analyser. The probe was held flat on the surface of the phantom. A minimum of ten measurements were taken from different locations on each individual tissue phantom, and averaged. In some cases, extra measurements were taken from inside the phantoms to ensure the mixtures' homogeneity.

The experimental result showing the relative permittivity variation with frequency for each of the four phantoms is given in Figure 1. The results for the gland and fat phantoms are shown in Figure 1a, along with the median of measurements on actual gland and fat tissue that were conducted in [5]. Figure 1b shows the permittivity for skin and tumour phantoms as well as the median from measurements of actual skin tissue (from [4], [6]) and actual malignant tissue (from [3]).

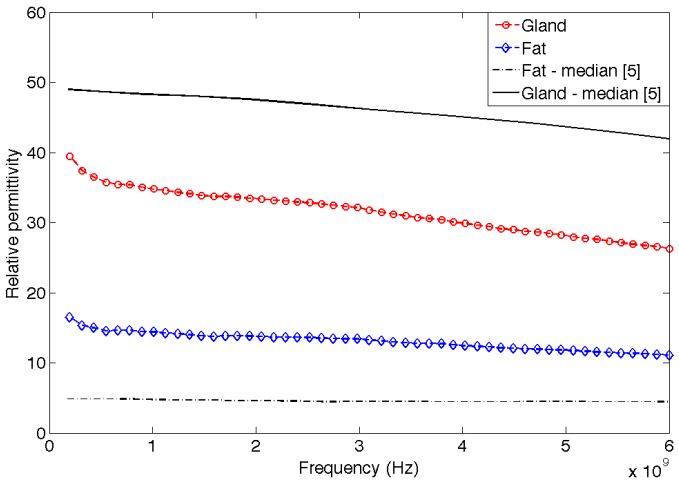

Fig. 1a Relative permittivity versus frequency for gland and fat tissue phantoms. Also shown is the median of the measurements conducted in [5] on actual gland and fat tissue.

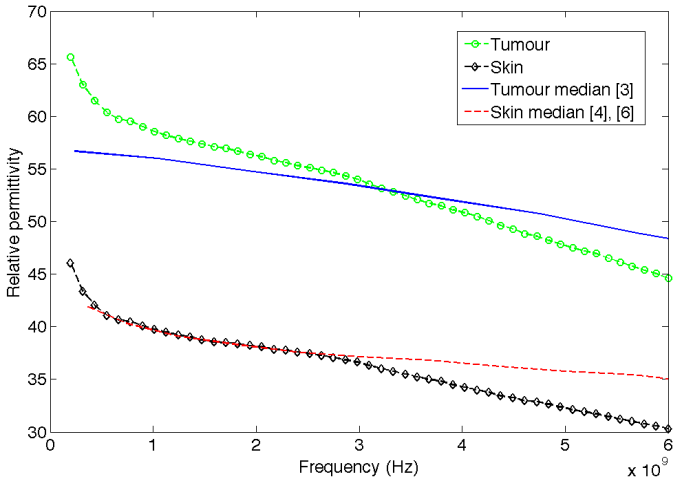

Fig. 1b Relative permittivity versus frequency for tumour and skin tissue phantoms. Also shown is the median of the measurements found in [3], [4] and [6] for actual tumour and skin tissue.

Similarly, the measured conductivity values at each frequency for the various phantoms are shown in Figure 2. As with the relative permittivity, first the results for gland and fat phantoms are plotted in Figure 2a. These are accompanied by the median conductivity found in measurements done on actual gland and fat tissue in [5]. Finally, Figure 2b shows the conductivity of the tumour and skin phantoms and the median of measurements of actual tumour and skin tissues [3], [4], [6].

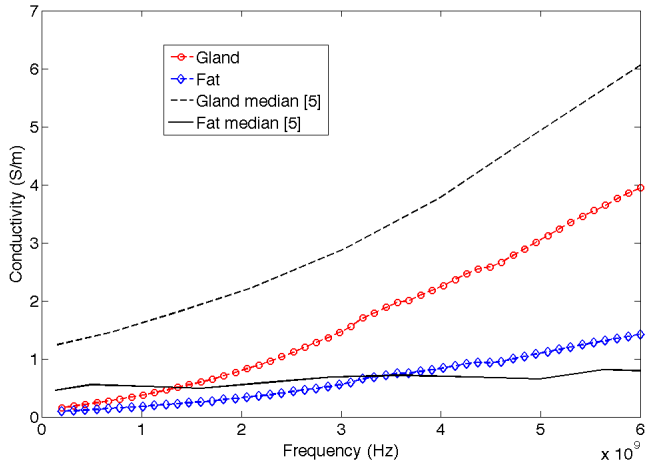

Fig. 2a Conductivity versus frequency for gland and fat tissue phantoms. Also shown is the median of the measurements conducted in [5] on actual gland and fat tissue.

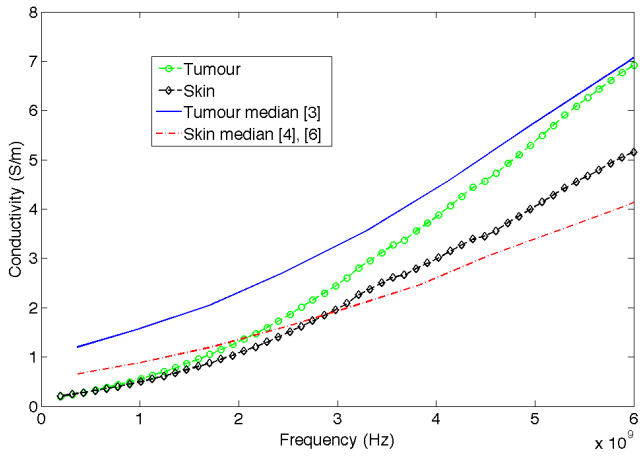

Fig. 2b Conductivity versus frequency for skin and tumour tissue phantoms. Also shown is the median of the measurements found in [3], [4] and [6] on actual skin and tumour tissue.

It is observed that the tumour phantom has, at worst, a deviation of 9 units of relative permittivity from the median of the measurements on actual malignant tissue reported in [3]. The gland phantom has a relative permittivity up to 15 units lower than the median of the gland tissue measured in [5], and the fat phantom's is up to 10 units lower than is measured in [5]. The skin phantom is the most closely matched to its corresponding measurements on actual skin tissue, here the phantom is 5 units away from the median relative permittivity given in [4], [6]. It may seem that the phantom's relative permittivities are not well matched to actual tissue types, but in fact for the tumour and gland phantoms, the relative permittivity is still within the range of values measured on actual tissue [5]. For instance, at 6 GHz, the gland phantom has a relative permittivity of 26, while the median measured value is just over 40 [5]. However, gland tissue measured at 6 GHz has a relative permittivity of anywhere from 20 to 35 [5], so clearly the gland phantom relative permittivity resides within this interval.

Thus for the skin, tumour and gland phantom, the difference from the desired values is tolerable, and certainly so when compared with the intrinsic variation of breast tissue properties within the breast and between different patients [3]. It is the fat phantom's relative permittivity which the least representative of actual fat tissue measurements; this will be discussed later. We also note the differences in conductivity between the phantoms and the median of actual tissue samples of 0.5 S/m, 2 S/m, 0.9 S/m and 1 S/m for fat [5], gland [5], tumour [3], and skin [4], [6], respectively.

When discussing the variations in dielectric properties between the tissue phantoms and actual tissue, there are two important points that must be mentioned. As stated above, tissue properties can vary widely between patients [3], so it is not necessary for tissue models to be an exact match to the measured quantities. Also, with the exception of the actual skin tissue, all of the measurements referred to have been those conducted on tissue first removed from the body [5], [3]. Recently, a study was published which concludes that in measurements conducted on excised tissue, the dielectric properties tend to decrease as compared to those of living tissue still in the body [7]. Ideally, our breast model should mimic the properties of living tissue that has not been removed, since a breast cancer detection system should be non-invasive. However for the purpose of phantom construction, it is more important to note that the variation in microwave dielectric properties for tissues is large and at present not definitively known, but the tissue phantoms should still approximate them as closely as possible.

The above results and discussion has focused on freshly made phantoms. Measurements were also made on a fat phantom that was six months old. The same mixture was used for both of the two fat phantoms. A comparison of the relative permittivity of the fresh fat and the older fat phantoms is shown in Figure 3. It is seen that the relative permittivity follows the same trend for both phantoms, however the old fat phantom has a relative permittivity about four points lower than the fresh fat. The conductivity, similarly, is lower in the older phantom. This brings the old fat phantom's relative permittivity and conductivity into the range expected for actual fat tissue by the studies in [3] and [5]. This observation guides our current work, which focuses on introducing a higher ratio of oil to gelatin in the fat phantom mixture in order to acquire the dielectric property range close to the one in the reported tissue measurement.

For most tests, however, the fresh fat phantom presented here is acceptable since it still leads to a significant contrast between tumour and fat. Here, we note that the contrast between tumour and fresh fat phantoms is 4:1 for relative permittivity and 5.5:1 for conductivity. The dielectric contrast between tumour and old fat is, correspondingly, 4.5:1 and 6:1.

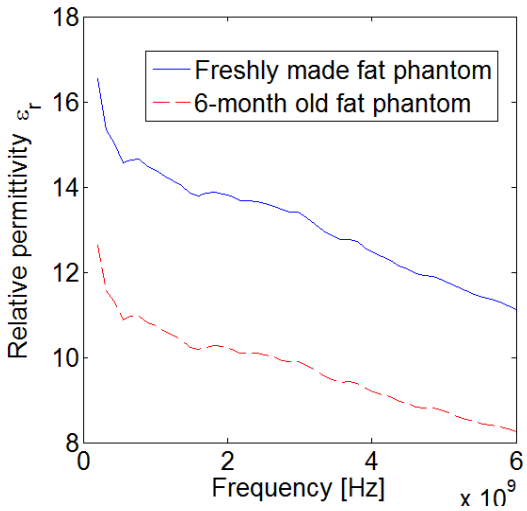

Fig. 3 Relative permittivity vs. frequency for freshly mixed and 6-month old fat-mimicking phantoms.

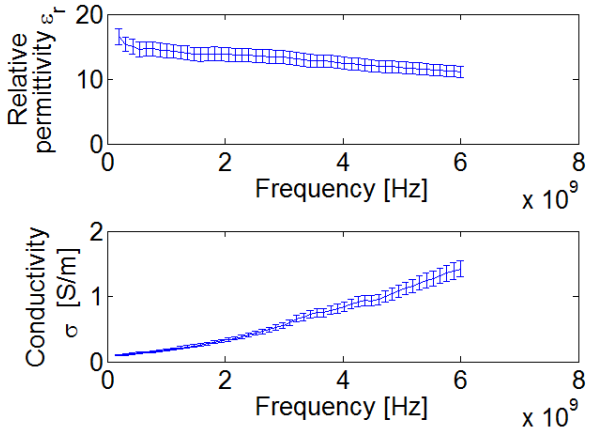

Fig. 4 Relative permittivity and conductivity vs. frequency for fresh fat-mimicking phantom showing standard deviation of measurements.

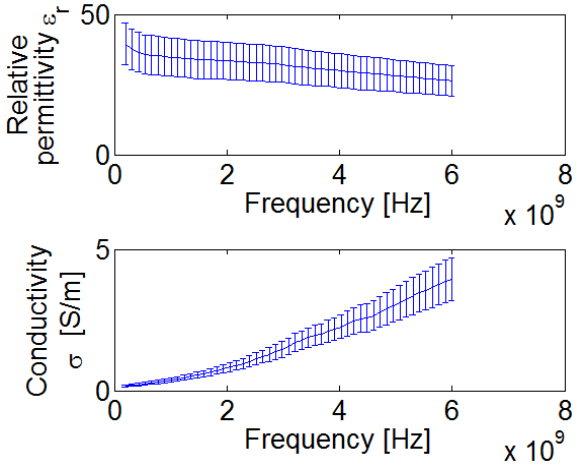

Fig. 5 Relative permittivity and conductivity vs. frequency for gland-mimicking phantom showing standard deviation of measurements.

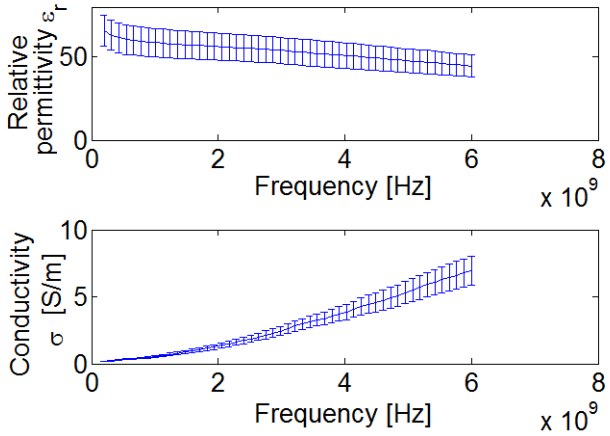

Fig. 6 Relative permittivity and conductivity vs. frequency for tumour-mimicking phantom showing standard deviation of measurements.

Figure 4 shows the average relative permittivity and conductivity of the fresh fat with the standard deviation of the measurements shown as error bars. Similarly, Figures 5, 6 and 7 show the variations in relative permittivity and conductivity versus frequency for the gland, tumour and skin-mimicking phantoms, respectively. It is noted that the variation in measurements does not have a negative effect on the overall results as the contrast between the tumour and fat would vary only slightly even with worst-case deviation.

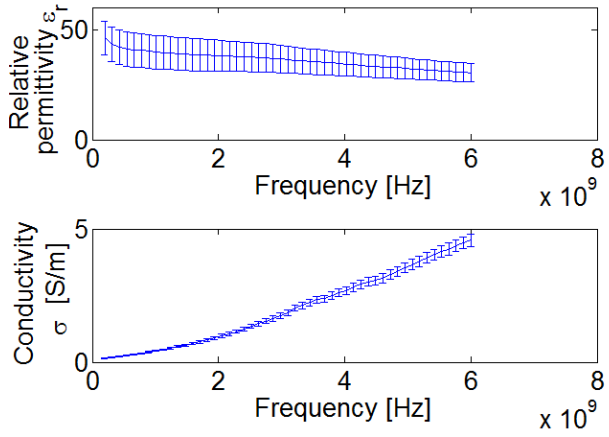

Fig. 7 Relative permittivity and conductivity vs. frequency for skin-mimicking phantom showing standard deviation of measurements.

C. Step 3: Building a Complete Breast Model

The four materials mimicking the breast tissues need to be merged into a model that, geometrically, matches the breast anatomy as realistically as possible. First, the 2-mm thick skin phantom is made by pouring the liquid skin mixture between two hemispherical bowls of strategically chosen radii. After the liquid mixture has had sufficient time to harden, the bowls can be separated. The practical challenges with this technique are: 1) difficulty in avoiding the formation of air pockets within the liquid when it is compressed between the two bowls and 2) the separation of the two containers can cause the skin phantom to tear. However, we found that compressing the liquid phantom very slowly between the two bowls avoids creating air pockets. As well, by pulling the bowls apart by applying equal pressure on all sides of the bowl it easy to separate them without tearing.

Once the skin has set, the fat phantom can be poured directly into it. If the breast model is to include one or more tumours, a batch of tumour mixture should be made ahead of time and allowed to solidify. Thereafter, the tumour phantom is easily cut into the desired shape and size. The fat-mimicking phantom can be poured into the hemispherical skin phantom in successive layers, enabling one or more tumour models to be placed at any location within the fat.

Incorporating the glands into the model is more challenging. Glands have approximately conical shape, with the narrower part of the cone being closer to the skin surface [8], [9]. To structurally mimic the glands within the phantoms, cylindrical glass rods were anchored in the fat before it solidified. Once the fat phantom hardens, the rods can be removed and the remaining hole can be carved out into a conical shape. At this point, the liquid gland mixture can be poured directly into the conical hole. This technique permits multiple gland models, and, further, for tumours to be placed within the glands.

Figure 8 shows an example of a resulting breast phantom with skin, fat, glands and tumour. The phantom has a radius of 6.5 cm, which is a realistic size. Two different gland structures are included. The smaller structure is all gland tissue, while the larger one contains a 1.5-cm tumour.

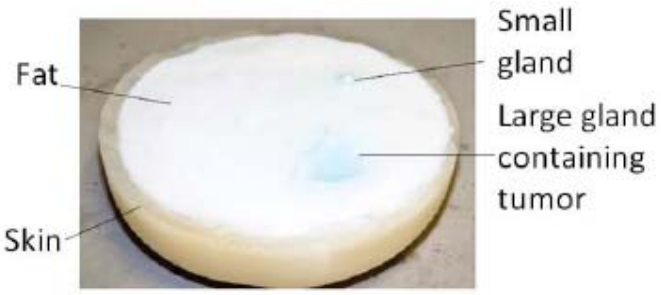

Fig. 8 Photograph of the complete breast phantom including skin, fat, glands and tumour.

III. Conclusions & Future work

In this paper, we have presented a method for constructing tissue phantoms with dielectric properties similar to those recently reported for breast tissue. Our procedure makes significant advances in physiological representation compared to the simplified models used to date, allowing for the inclusion of multiple conical-shaped glands of varying size and the placement of tumours within these glands. Four phantoms were made with characteristics that approximate the permittivity and conductivity of actual breast fat, gland, skin and tumour tissue. Measurements were performed on each phantom type to verify that the conductivity and permittivity are appropriate. Finally, a complete breast model was assembled which incorporated the four different tissue phantoms in a distribution pattern representative of the human breast anatomy. For parametric studies, the contrast between healthy and malignant tissues can be controlled by changing the concentration of oil in the tumour phantom. This overall phantom offers a comprehensive breast model that is suitable for validation experiments on microwave breast cancer detection.

Acknowledgment

The authors would like to thank Mr. Jules Gauthier of the Centre PolyGrames at the Université de Montréal for his laboratory help with the tissue measurements. We are grateful to Mr. Donald Pavlasek of the Electrical & Computer Engineering Department at McGill University for the construction of the moulds needed for the phantoms. Last but not least, the authors would like to acknowledge the support of the following funding agencies: Natural Sciences and Engineering Research Council of Canada (NSERC), Fonds de recherche sur la nature et les technologies (FQRNT), and Partnerships for Research on Microelectronics, Photonics and Telecommunications (PROMPT).

References

[1] E.C. Fear, "Microwave Imaging of the Breast," *Technology in Cancer Research and Treatment*, Vol. 4, no.1, pp. 69-82, 2005.

[2] M. Lazebnik, L. McCartney, D. Popovic, C. Watkins, M. Lindstrom, J. Harter, S. Sewall, A. Magliocco, J. Booske, M. Okoniewski and S. Hagness, "A large-scale study of the ultrawideband microwave dielectric properties of normal breast tissue obtained from reduction surgeries," *Phys. Med. Biol.*, Vol. 52, pp. 2637-2656, 2007.

[3] M. Lazebnik, D. Popovic, L. McCartney, C. Watkins, M. Lindstrom, J. Harter, S. Sewall, T. Ogilvie, A. Magliocco, T. Breslin, W. Temple, D. Mew, J. Booske, M. Okoniewski, and S. Hagness, "A large-scale study of the ultrawideband microwave dielectric properties of normal, benign and malignant breast tissues obtained from cancer surgeries," *Phys. Med. Biol*., Vol. 52, pp. 6093-6115, 2007.

[4] M. Lazebnik, E. Madsen, G. Frank and S. Hagness, "Tissue-mimicking phantom materials for narrowband and ultrawideband microwave applications," *Phys. Med. Biol.,* Vol. 50, pp. 4245-4258, 2005.

[5] E. Zastrow, S. Davis, M. Lazebnik, F. Kelcz, and S. Hagness, "Development of Anatomically Realistic Numerical Breast Phantoms With Accurate Dielectric Properties for Modeling Microwave Interactions With the Human Breast," *IEEE Transactions on Biomedical Engineering*, Vol. 55, no.12, pp. 2792-2800, 2008.

[6] S. Gabriel, R.W. Lau and C. Gabriel, "The dielectric properties of biological tissues: II. Measurements in the frequency range 10 Hz to 20 GHz," *Phys. Med. Biol.,* Vol. 41, pp. 2251-2269, 1996.

[7] R. J. Halter, T. Zhou, P.M. Meaney, A. Hartov, R.J. Barth Jr, K.M. Rosenkranz, W.A. Wells, C.A. Kogel, A. Borsic, E.J. Rizzo and K.D. Paulsen, "The correlation of *in vivo* and *ex vivo* tissue dielectric properties to validate electromagnetic breast imaging: initial clinical experience," *Physiol. Meas*., Vol. 30, pp. S121-S136, 2009.

[8] (2009) Canadian Cancer Society, "What is breast cancer?" [Online]. Available: http://www.cancer.ca/

[9] A.C. Guyton, J.E. Hall, *Textbook of Medical Physiology*, 11th ed., Saunders, 2005.